



universität  
wien

BACHELOR'S THESIS

# **Evolution and Escape of Atmospheres of Planets orbiting M dwarfs**

*Schleich Simon*

supervised by  
Dr. Kristina G. KISLYAKOVA

Submission Date: August 29, 2019

## Abstract

The question if planets outside our solar system could have the possibility to sustain life on their surface goes hand in hand with the recent discovery of thousands of exoplanets, a fraction of which are terrestrial and could therefore possess environments similar to these of the Earth. While it would be natural to search for habitable planets around stars like our Sun, the abundance of M dwarfs in the galaxy together with their incredibly long lifetimes and their advantages in terms of discovering exoplanets makes them prime targets for exoplanet discovery missions such as TESS. However, planets in the habitable zone around M dwarfs experience an environment completely different to Earth, linked to the strong stellar magnetic fields and long activity lifetimes. These factors influence the possibility of an exoplanet to retain its vital atmosphere, which might be stripped away in the blink of an eye, speaking in cosmic timescales.

Analyzing a sample of M dwarfs, this thesis concludes that an Earth-like planet with an atmospheric composition dominated by nitrogen could not sustain its atmosphere in the habitable zone of any of the stars in this sample over significant amounts of time because of the high X-ray and Extreme Ultraviolet (XUV) fluxes these stars provide for their planetary companions. Planets around M dwarfs would have to survive being exposed to extreme stellar environments for prolonged periods of time before the host stars might present stable conditions for an atmosphere.

# Contents

<b>1</b>	<b>Introduction</b>	<b>1</b>
<b>2</b>	<b>Exoplanets and habitability</b>	<b>3</b>
2.1	Atmospheric structure . . . . .	3
2.2	Formation of atmospheres . . . . .	4
2.3	The habitable zone . . . . .	6
<b>3</b>	<b>M dwarf stars</b>	<b>8</b>
3.1	Influence on exoplanet atmospheres . . . . .	8
3.1.1	Effects of proximity . . . . .	10
<b>4</b>	<b>Atmospheric loss estimation</b>	<b>12</b>
4.1	Computational background . . . . .	12
4.2	Results . . . . .	14
<b>5</b>	<b>Conclusion</b>	<b>20</b>
	<b>References</b>	<b>29</b>

## 1 Introduction

M dwarfs, or dM stars, are the most abundant stars in our galaxy (Scalo et al. 2007), which should make them at least statistical prime candidates for the detection of planets with the potential environmental conditions for habitability. That being said, they are very different from our Sun and distinguish themselves through, amongst other things, a very long active phase in their life cycles (West et al. 2008) marked by strong stellar magnetic fields and winds as well as the release of large amounts of high energy radiation (Scalo et al. 2007; Shields et al. 2016). All this can create hostile environments for planets orbiting in their habitable zones, which are situated very close the host star given the fact that M dwarfs are very faint when compared to the Sun (Scalo et al. 2007; Kopparapu et al. 2013).

To be considered habitable, a planet should be able to sustain liquid water on its surface, which is often used to confine an area around a star called the *habitable zone* where this is possible (Selsis et al. 2007). Having an atmosphere is also a requirement for habitability in this sense, and the influences an M dwarf as a host can have on the atmospheres of potential exoplanets in orbit around them might prevent these atmospheres from being retained over a significant amount of time (Lichtenegger et al. 2010). High amounts of incident XUV radiation (in a range of about 1 - 1000 Å) coming from the active stellar hosts are absorbed in the upper layers of a planet's atmosphere, causing the thermal escape of atmospheric constituents as well as the expansion of the atmosphere (Tian et al. 2008). A strong stellar magnetic field, as it can be found in dM stars, pushes the planetary magnetosphere close to the planet itself (Vidotto et al. 2013), which coupled with the expansion process exposes the atmosphere to the detrimental effects of the stellar wind. Ionized atmospheric particles are dragged away by the propagating interplanetary magnetic field, ejected from the atmosphere through collisions or vanish along the open field lines at the planets' magnetic poles (Lichtenegger et al. 2010; Vidotto et al. 2013; Kislyakova et al. 2014). Even the proximity of the habitable zone to an M dwarf itself could render a potential planet uninhabitable, caused by extreme volcanism through tidal forces or induction-induced heating (Barnes et al. 2013; Kislyakova et al. 2018). However, while dM stars go through an extended phase of high stellar activity, they show no significant brightening along the main sequence (Scalo et al. 2007) and the lower mass M dwarfs never evolve into red giants (Laughlin et al. 1997), potentially providing stable exoplanet environments for their very long lifetimes.

Keeping all this in mind, dM stars are valued targets for scientific missions with the goal of discovering exoplanets. Together with the CoRoT satellite (*Convection, Rotation and planetary Transits*), which was launched in 2006 and discovered 34 exoplanets (CoRoT 2016), the probably most well known scientific mission with the goal of identifying Earth-like planets around main-sequence stars was Kepler, launched in 2009 (Johnson 2018). While exoplanets can and have been detected through a number of different methods, including the measurement of doppler-shifted stellar spectral lines due to the movement of a star and its planet around their common center of mass (Doppler spectroscopy), about 75% of the confirmed exoplanets to date have been detected via the transit method (Exoplanet Catalogue 2019). Using the transit method, an exoplanet can be indirectly

observed by monitoring the stellar light curve of its host star. As the planet passes in front of it, the resulting dip in the stellar light curve then allows the identification of a number of parameters of the planet-star system, such as the orbital distance of the planet by considering its orbital period, as well as its size through the measurement of the depth of the transit. Since transits only last for very short periods of time, continuously monitoring stars increases the probability of the detection of an exoplanet. This fact, combined with considerations on the highest number of star to observe, lead to the selection of a rather small and fixed field of view for the four-year primary Kepler mission from 2009 to 2013 ([Johnson 2018](#)). Together with its secondary mission K2, which started in 2013 and lasted until 2018, Kepler has discovered 2,725 exoplanets and identified 2,955 further candidates ([NASA Exoplanet Archive 2019](#)).

While Kepler observed a fixed field of view over an extended period of time, the scientific goal of the *Transiting Exoplanet Survey Satellite* is an all-sky survey in the search for transiting exoplanets ([Ricker et al. 2016](#)). TESS was launched on April 18, 2018 and will spend two years scanning first the southern and then the northern hemisphere of the sky, each separated into 13 segments that are observed for about 27 days respectively, with regions near the ecliptic poles showing an overlap of segments that results in viewing times of up to 100 days, increasing the likelihood of a transit observation in these regions. On board TESS are four identical wide-field cameras that use a bandpass between 600 and 1000 nm, which makes them ideal for observing not only solar-like, but also cooler types of stars such as M dwarfs, which give off most of their light beyond the visible spectrum ([TESS 2019](#)). As of writing this, 20 exoplanets have been discovered by TESS and 487 candidates already await confirmation ([Exoplanet Catalogue 2019](#)), though by observing around 200,000 stars in total, TESS is estimated to identify between 500 and 1,000 earth- and super-earth sized exoplanets ([Cooper 2018](#)).

## 2 Exoplanets and habitability

At the time of writing this, close to 4100 exoplanets have been confirmed orbiting in about 3000 planetary systems ([Exoplanet Catalogue 2019](#)). A question that arises naturally following this huge number of discovered worlds is, if life might exist on some of these planets or at least if their environment would potentially allow its evolution and extended existence. In the search for planets that could allow this, the notion of a *habitable zone* refers to a circumstellar region in which life as we know it could be possible on a planet. Since this would be a very broad definition of the term itself, the habitable zone is generally defined as the region around a star in which a terrestrial-mass planet with an atmosphere similar to Earth's could sustain liquid water on its surface ([Scalo et al. 2007](#); [Selsis et al. 2007](#); [Kopparapu et al. 2013](#)). Stellar insolation plays a major role in this, though other mechanisms can also control, or at least influence, the temperature on the planetary surface, such as tidal forces ([Barnes et al. 2013](#)). The overall existence of an atmosphere surrounding the planet combined with the changes it experiences as a result of a variety of different influencing parameters is an important factor when considering the habitability of an exoplanet.

### 2.1 Atmospheric structure

The atmosphere of a planet is a gaseous envelope that surrounds the planet. The vertical temperature distribution in Earth's atmosphere allows a separation into several different layers as described in [Bauer & Lammer \(2004, p. 3ff.\)](#):

Starting from the surface, the first layer of the atmosphere is called the troposphere. It is characterized by a negative temperature gradient that terminates at the tropopause at a height of about 13 km and reverts into a positive gradient in the stratosphere as a result of the absorption of UV radiation by ozone. The stratosphere terminates at the stratopause, about 50 km from the surface, after which the temperature gradient again becomes negative in the next layer, called the mesosphere. After the termination of the mesosphere at the mesopause at a height of around 85 km, the absorption of X-ray and EUV radiation (from here on XUV) leads to a steep increase in temperature corresponding to altitude in the next atmospheric layer, called the thermosphere. Beyond sufficient heights, the mean free paths between atmospheric constituents become large enough to disregard collisions between them, which is when the thermosphere terminates at the thermopause and the last layer of the atmosphere is reached, called the exosphere. Some particles in the exosphere in the high-energy end of the Maxwellian distribution can reach velocities that exceed the escape velocity of Earth leading to the atmospheric loss into space.

Two more definitions should also be mentioned when talking about Earth's atmosphere and its interaction with the solar environment. The term ionosphere describes the parts of the atmosphere where the ionization fraction is high as a result of the absorption of X-ray and EUV radiation and from the interaction with high energy particles such as cosmic rays and the solar wind. The magnetosphere on the other hand is the region of influence of the planetary magnetic field and terminates at the magnetopause. Because

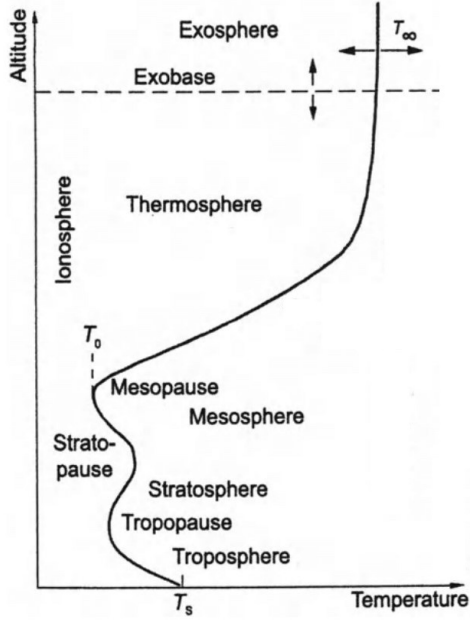


Figure 1: Temperature distribution with respect to altitude and corresponding terrestrial designations of atmospheric layers, showing the more compact regions below the thermosphere, as well as the more expansive upper regions, together with their corresponding transition regions.  $T_s$  marks the temperature at the planetary surface,  $T_0$  the temperature at the base of the thermosphere and  $T_\infty$  the constant temperature reached at the exobase (Image from [Bauer & Lammer \(2004, p. 4\)](#), altered).  $T_\infty$  as well as the height of the exobase vary with different amounts of incident XUV flux ([Tian et al. 2008](#)).

of the interaction between the planetary magnetic field and the solar wind, the shape of the magnetosphere is not circular but rather differs for Earth's day- and nightside ([Bauer & Lammer 2004, p. 5f](#)).

These definitions of the atmospheric layers are also used to describe the atmospheres of the other planets in our solar system, and they also naturally serve as indicators for the atmospheres of exoplanets outside our solar system.

## 2.2 Formation of atmospheres

To provide an environment that could allow a planet to sustain liquid water on its surface, it should possess an atmosphere that regulates its surface temperature. However, such an atmosphere is not the first gaseous envelope that forms around a developing planet. During the planetary formation phase, gas from the protoplanetary disk is gravitationally accreted onto the planetary embryos or protoplanets which forms a first gaseous envelope around the planetary precursor ([Lammer et al. 2018](#)). This *primary atmosphere*, mostly consistent of  $H_2$ , escapes when the protoplanetary disk disappears

since light atmospheric constituents such as hydrogen readily escape through thermal and non-thermal mechanisms ([Zahnle et al. 2010](#)).

During the formation of a planet, meteorites containing water-, nitrogen- and carbon-bearing materials might be accreted, determining the initial volatile inventory of the planet ([Zahnle et al. 2010](#)). The energy sources during the planetary formation, like heating caused by the decay of short-lived radioactive isotopes, can be high enough to create magma ponds or even global magma oceans on the planet that solidify from the bottom to the top, expelling the non-solidifying volatile inventory including  $\text{H}_2\text{O}$ ,  $\text{NH}_3$  and carbon compounds such as  $\text{CO}_2$  in a process called outgassing ([Elkins-Tanton 2012](#)), leading to the formation of a *secondary atmosphere*.

However, this atmosphere is not formed by the static accumulation of the outgassed molecules, but develops through the properties of these volatiles and their interactions with their surroundings. When looking at the nitrogen-dominated atmosphere of an Earth-like exoplanet it is reasonable to relate its evolution to the development of Earth's atmosphere, where the majority of the expelled volatiles were made up of water vapour, while Earth's current atmosphere is dominated by nitrogen ([Renneboog & Boorstein 2013](#), p. 51).

A major contributor to these changes is the breakdown of atmospheric molecules into sub-compounds through the absorption UV photons, in a process called photodissociation.



Examples for this include the photolysis of nitrogen ( $\text{N}_2$ ) from ammonia ( $\text{NH}_3$ ) and of hydroxyl radicals ( $\text{OH}$ ) from water molecules ( $\text{H}_2\text{O}$ ) ([Lammer et al. 2018](#)). Next to photodissociation and the ensuing escape of light atmospheric constituents, the depletion of expelled  $\text{H}_2\text{O}$  and  $\text{CO}_2$  from the atmosphere also occurs along with the formation of oceans due to the saturation of water vapour in the atmosphere and subsequent condensation of further outgassed  $\text{H}_2\text{O}$  ([Renneboog & Boorstein 2013](#), p. 51). The carbon dioxide reacts with water molecules to form carbonic acid ( $\text{H}_2\text{CO}_3$ ), which dissociates into bicarbonate ( $\text{HCO}_3^-$ ) and hydrogen ions and is subsequently bound in sediments on the seafloor ([Lammer et al. 2018](#)).

This leaves nitrogen originating from the photolysis of ammonia, which built up to be the dominant atmospheric constituent because it is almost chemically inert, relatively insoluble in water and does not condense out of the atmosphere ([Renneboog & Boorstein 2013](#), p. 52), leading to the formation of the nitrogen-dominated atmosphere present on Earth today. The second most abundant component of Earth's atmosphere, oxygen, saw its rise as a byproduct of the advent of microbial life and photosynthesis, as did the atmospheric ozone, which chemically forms from oxygen and shields organisms from the biologically damaging influences of stellar UV radiation ([Lammer et al. 2018; Renneboog & Boorstein 2013](#), p. 53). This implies that oxygen might not be as present in the atmospheres of Earth-like exoplanets, leaving them with a stronger presence of  $\text{CO}_2$  and  $\text{H}_2\text{O}$  caused by the missing photosynthetic conversion process.

### 2.3 The habitable zone

As mentioned above, the habitable zone of a star is a key factor when searching for potentially habitable planets. However, a planet orbiting in this region is not necessarily habitable since its surface temperature, governed by the distance to the host star and, therefore, the amount of radiation received by the planet, is not the only parameter influencing the planetary habitability ([Selsis et al. 2007](#)). Nevertheless, estimating the distance of the habitable zone through incident stellar irradiation allows the assessment of other factors that influence the planetary habitability depending on the separation between the star and the planet, such as the possible loss of an atmosphere.

Establishing the inner and outer boundaries of the habitable zone is based on the confining assumptions granting the habitability of the planet. [Selsis et al. \(2007\)](#) illustrated a pair of conservative and a pair of more optimistic assumptions as follows:

- a) The conservative assumptions are based on the influences of greenhouse gases on the surface temperature of the planet. For the inner edge, [Selsis et al. \(2007\)](#) argued that an atmosphere dominated by water vapour (the amount of which in the atmosphere increases at closer orbits due to the increasing surface temperature) experiences a positive feedback loop in which the rising IR-opacity of the atmosphere leads to the reduction in cooling for the planet, which in turn expels more water vapour into the atmosphere, until a point is reached where the whole water inventory of the planet is vaporised, effectively making it inhospitable.

The arguments for the outer edge from [Selsis et al. \(2007\)](#) are based on an atmosphere dominated by CO<sub>2</sub>, where the interplay between the increasing planetary albedo, the incident solar flux and the increasing IR opacity leads to a maximum distance at which the greenhouse effect can sustain surface temperatures needed for liquid water, beyond which the planet would effectively freeze out.

- b) The more optimistic confining assumptions are based on empirical indications of the edges of the habitable zone. The arguments given by [Selsis et al. \(2007\)](#) are based on observations that suggest 1) that there has been no liquid water on Venus for at least 1 Gyr and 2) that Mars might have had liquid water on its surface 4 Gyr ago. Scaling the solar luminosity according to these times and the distances of Venus and Mars to the Sun results in the empirical *recent venus* and *early mars* criteria.

A way to determine the distance of the habitable zone to its host star was given by [Kopparapu et al. \(2013\)](#). They used a 1D, convective-radiative and cloud-free climate model to determine the edge of the habitable zone closest to and furthest away from the Sun. By expanding their model to main-sequence stars in a temperature range between 7200 and 2600 K they also allowed the calculation of the habitable zone for the spectral types F through M. The equation derived by [Kopparapu et al. \(2013\)](#) following the criteria outlined above is given below, where  $l$  describes the distance to the star,  $L$

denotes the stellar luminosity and  $T_s = T_{\text{eff}} - 5780$  is a corrected stellar temperature.

$$l = (S_{\text{eff},\odot} + aT_s + bT_s^2 + cT_s^3 + dT_s^4)^{-\frac{1}{2}} \left( \frac{L}{L_{\odot}} \right)^{\frac{1}{2}} \quad [\text{AU}] \quad (2.2)$$

Later, Kopparapu et al. (2014) improved the equation by taking the planetary mass into account. Knowing the distance of the habitable zone to a host star is important when looking at the possible influences said star can have on the atmospheres of planets in orbit around them. Some of these influences are discussed in Section 3.1.

### 3 M dwarf stars

M dwarfs are cool, low mass and low luminosity stars that can be found on the lower end of the main sequence. With masses in a range between  $\sim 0.08\text{--}0.6 M_{\odot}$  and temperatures between 2300 and 3800 K (Reid & Hawley 2005, p. 169), the stars themselves and the environments they create for possible planetary companions are significantly different when compared with solar-like stars. Following Wien's displacement law, M dwarfs produce most of their light in the IR-part of the electromagnetic spectrum, and even the brightest among them are about 10 times fainter than the Sun, with luminosities decreasing to below  $10^{-3} L_{\odot}$  (Scalo et al. 2007) for the latest spectral types. Speaking in terms of general absolute values, the energies released from these stars are therefore lower in comparison to our Sun, but a major concern when talking about the potential habitability of planets is their distance to the host star of the system, and since M dwarfs are that much fainter than other main sequence stars, their habitable zones are situated much closer to the star itself, roughly following the relation  $l \propto L^{1/2}$  (Kopparapu et al. 2013) when comparing the distance  $l$  in AU with the stellar luminosity  $L$  in terms of solar luminosity (for a more thorough discussion see Section 2.3).

Therein lies one of the problems concerning the habitability of exoplanets in M dwarf systems. While the peak of their energy distribution is shifted into the IR, they show an increased amount of short wavelength XUV radiation due to stellar activity on timescales of up to a few Gyr for the later spectral types (West et al. 2008). Figure 2 illustrates this by comparing the short wavelength flux between our modern Sun and an active young Sun of a distance of 1 AU, as well as the flux from the M dwarf GJ 832 at a distance of 0.162 AU, where an exoplanet has been found in the habitable zone (Exoplanet Catalogue 2019). While the flux around GJ 832 is significantly lower above 150 nm as would be expected from a fainter and cooler star, the flux in the XUV spectral range up to about 100 nm is more comparable to an active Sun. This means that even though M dwarfs can reach main sequence lifetimes of up to  $10^{13}$  years (Laughlin et al. 1997), they might only provide reasonable environments for planets in their habitable zones after these planets have spent a significant amount of time, up to several Gyr for lower mass stars in this spectral type (West et al. 2008), being exposed to the effects of stellar activity, which include increased incident XUV radiation from flaring as well as interactions with high energy particles from stellar winds and possible CMEs (coronal mass ejections) (Scalo et al. 2007; Lichtenegger et al. 2010). This has detrimental consequences for the atmospheres that these planets have to sustain for them to maybe be considered habitable.

#### 3.1 Influence on exoplanet atmospheres

A planet might lose its atmosphere through a number of different mechanisms as a result of influences from its host star, which can be separated into thermal and non-thermal escape processes (Catling & Zahnle 2009).

Thermal escape happens as a result of heating processes in the upper layers of a planetary atmosphere. Assuming that the velocity of the atmospheric constituents follows a

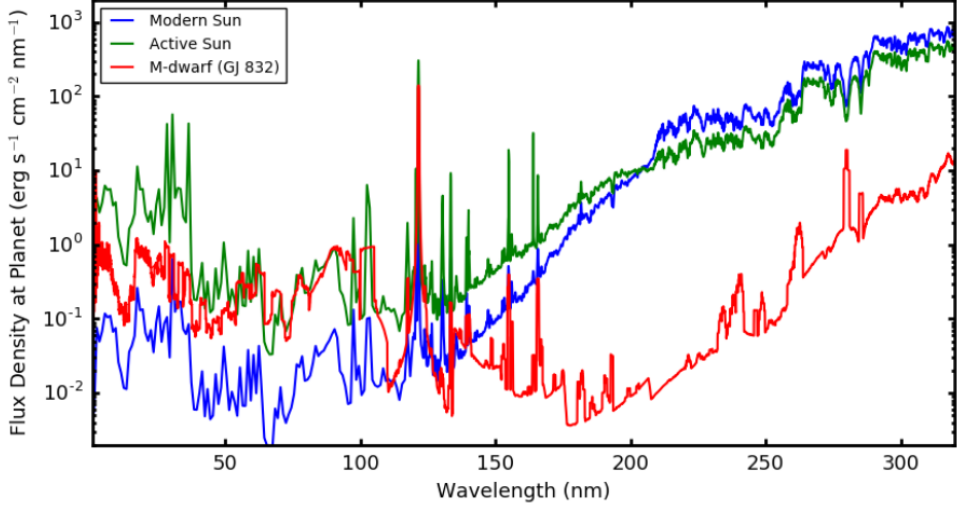


Figure 2: Example spectra to compare the flux density in the XUV regime of the respective stellar spectra for our modern sun (blue) and an active sun (green) at a distance of 1 AU (Claire et al. 2012), as well as for the M dwarf GJ 832 at a distance of 0.162 AU (Fontenla et al. 2016) where a planet in the habitable zone has been discovered (Exoplanet Catalogue 2019).

Maxwellian distribution, particles at the upper tail of the distribution might exceed the planetary escape velocity and therefore leave the planet, not being impeded by collision in the exosphere, in a process called *Jeans escape* (Tian et al. 2008). If the temperatures reach sufficiently high levels, Jeans escape can turn into a process called *blow-off* or *planetary wind*, where the atmospheric constituents leave the atmosphere in a bulk flow, bringing it into the hydrodynamic regime (Tian et al. 2008; Catling & Zahnle 2009). As pointed out by Lichtenegger et al. (2010), the hydrodynamic blow-off of atmospheric hydrogen starts at a temperature of  $\sim 5000$  K, and the hydrostatic regime of an atmosphere dominated by nitrogen and oxygen cannot be maintained above a temperature of  $\sim 8000$  K. Tian et al. (2008) modelled the temperature at the exobase of an Earth-like atmosphere with respect to high amounts of incident XUV radiation, reaching almost  $1 \times 10^4$  K for levels of about  $6.6F_0$ , where  $F_0$  represents the current solar value (taken to be  $\sim 5.1 \text{ erg s}^{-1} \text{ cm}^{-2}$  in their case). After this maximum, the exobase temperature decreased in their model, ranging up until  $20F_0$ , which was caused by adiabatic cooling effects (Tian et al. 2008), although as pointed out by Johnstone et al. (2019), at even higher XUV fluxes ( $60F_0$  in their respective case) the heating caused by the input XUV radiation begins to surpass the cooling effects. Next to the heating-induced loss, the expansion of the thermosphere is another effect of the absorption of XUV radiation, which becomes important when looking at non-thermal atmospheric loss.

Besides the thermal loss, several non-thermal processes can also severely impact the evolution of a planets atmosphere. The ionization of atmospheric constituents plays a

major role in these mechanisms. This can happen e.g. through the photoionization of the major atmospheric constituents as a result of the absorption of stellar XUV radiation (Bauer & Lammer 2004, p. 11), as well as through electron-impact and charge-exchange ionization, which are strongly influenced by the interaction between the atmosphere and the stellar wind (Lichtenegger et al. 2010). The non-thermal loss itself then happens through a number of different processes. One of these is the *polar flow*, describing the escape of ions along the open magnetic field lines at the magnetic poles of a planet, which originate due to the interaction between the planetary magnetic field and the stellar wind plasma (Vidotto et al. 2013). Sputtering is another loss process and represents the collision-based energy transfer between e.g. solar wind protons and atmospheric particles, ejecting them either directly or through a cascade of collisions (Bauer & Lammer 2004, p. 69f). Being exposed to the stellar wind, ions can also be picked up and whisked away from a planet by the propagating interplanetary magnetic field, which is carried by the stellar wind, in the aptly named *ion pick-up* process (Kislyakova et al. 2014). In the case of Earth today, the planetary magnetic field protects the upper layers of the atmosphere from the strong erosion effects of the solar wind by maintaining a magnetopause at around  $10 R_\oplus$ , while the exobase resides at levels significantly below that (Lichtenegger et al. 2010; Vidotto et al. 2013). However, the different environment for planets in orbit around M dwarfs can change this. Vidotto et al. (2013) have shown that an Earth-like planet orbiting a dM star with a magnetic field two to three orders of magnitude stronger than our Sun's would show a magnetospheric size several times smaller than Earth's current magnetosphere. Coupled with the expansion of the thermosphere through increased incident XUV radiation mentioned above, this could realistically lead to the exposure of the upper atmospheric layers to the detrimental effects of the stellar wind and therefore to high amounts of atmospheric loss.

Another possibility for atmospheric loss that should be mentioned here, but will not be further discussed since it is mainly relevant for young planets, is the so-called process of *impact erosion* caused by the collision of large bodies with an exoplanet (Catling & Zahnle 2009).

### 3.1.1 Effects of proximity

The stellar activity that defines the in part extreme environments exoplanets experience in the habitable zone of M dwarfs is not the only influencing factor on these planets that distinguishes them in their position around their host star. The afore mentioned proximity of the habitable zone to the M dwarf host also plays a role in shaping the environment that potential planets orbit in.

One of the effects this can have on an exoplanet was discussed by Barnes et al. (2013), who reviewed the influences that tidal heating can have on the habitability of exoplanets. Tidal heating due to varying gravitational forces can drive volcanic activity and the outgassing of volatiles, and they concluded that tidal heating could instigate a runaway greenhouse effect on planets with eccentric orbits, even if they would reside within the inner boundary of the conservative habitable zone as discussed in Section 2.3.

Another instigator for volcanic activity could be a varying magnetic field and the subse-

quent production of heat through Joule heating, resulting from the passing of induction-induced currents through a conductor, in this case the planet. [Kislyakova et al. \(2018\)](#) discussed the energy generated in an Earth-like exoplanet around strongly magnetized stars and they concluded that the energy generated through this process, depending on the distance to the star and the conductivity of the planetary mantle, likely leads to extreme volcanism and therefore increased outgassing of volatiles from the planetary interior. Next to driving a possible greenhouse effect, this could also provide mitigating effects on the atmospheric loss, although [Lammer et al. \(2018\)](#) compared the nitrogen loss rates determined by [Lichtenegger et al. \(2010\)](#) with current volcanic outgassing of nitrogen and concluded that even outgassing rates 20 times higher than today could not mitigate the nitrogen loss.

Other effects of the habitable zone proximity that might add problems for the habitability of exoplanets in orbit around M dwarfs also exist, such as synchronous rotation or the less constrained case of tidal locking ([Barnes et al. 2013](#)), but will not be discussed here.

## 4 Atmospheric loss estimation

Using a sample of 159 dM stars given by [Stelzer et al. \(2013\)](#) together with simplified assumptions about the conditions of a potential Earth-like planet orbiting these stars (given an atmosphere that is dominated by nitrogen and therefore comparable to Earth's atmosphere today), estimations about the loss of atmospheric nitrogen can be made as presented below, based on X-ray observations of these stars and a simplified scaling of their EUV spectra.

### 4.1 Computational background

The necessary stellar parameters to compute the loss of atmosphere for an Earth-like planet are given by [Stelzer et al. \(2013\)](#), with an example of a few stars shown in Table 1. They determined the X-ray flux in a range between  $\sim 0.6 - 6$  nm (equivalent to energies of 2 - 12 keV) by comparing the data from several catalogues to a 10 pc sample of bright M dwarfs. Using the distance to the star, the bolometric and X-ray luminosities  $L_{\text{bol}}$  and  $L_X$  can be calculated from the flux values, with  $r$  corresponding to the distance and  $F$  to the respective flux values.

$$L = 4\pi r^2 F \quad [\text{erg s}^{-1}] \quad (4.1)$$

To determine the amount of incident radiation and therefore the atmospheric loss, a distance for the planet to orbit the star has to be set. Since this is an estimation for the atmospheric loss of a potentially habitable planet, the orbit of said planet is set in the host stars habitable zone. A way in which the distance of the habitable zone around main sequence stars has been estimated has already been described in Section 2.3, so the computation of this distance follows Equation 2.2. Since the planet in this case is taken to be an Earth-equivalent, the parameters listed in Table 2 have been chosen corresponding to  $1M_\oplus$ . As illustrated by [Johnstone et al. \(2019\)](#), in the case of large amounts of incoming high-energy XUV-radiation the atmosphere is lost through a transonic hydrodynamic outflow, where the resulting loss rates can be described with the equation for energy-limited hydrodynamic loss.

$$\dot{M} = \frac{\epsilon\pi F_{\text{XUV}} R_{\text{pl}} R_{\text{XUV}}^2}{GM_{\text{pl}}} \quad [\text{g s}^{-1}] \quad (4.2)$$

$F_{\text{XUV}}$  describes the incident XUV flux on the planet,  $R_{\text{pl}}$  and  $M_{\text{pl}}$  planetary radius and mass,  $\epsilon$  the mass-loss efficiency and  $R_{\text{XUV}}$  the radius at which the incoming radiation is absorbed. Assuming an Earth-equivalent planet and simplified conditions, the parameters are set to  $R_{\text{pl}} = R_\oplus$ ,  $M_{\text{pl}} = M_\oplus$ ,  $\epsilon = 1$  and  $R_{\text{XUV}} = R_{\text{pl}}$ . Assuming a nitrogen-dominated atmosphere, the mass loss represented in Equation 4.2 can be adopted as a rate for nitrogen loss. It should be noted that this equation cannot be used to describe hydrostatic atmospheres since it strongly overestimates loss rates (resulting in  $10^7 \text{ g s}^{-1}$  for modern Earth's values) and should therefore only be used to estimate the loss of hydrodynamic atmospheres.

Name	Spectral Type	$T_{\text{eff}}$ [K]	d [pc]	$\log F_{\text{bol}}$ [ $\text{erg/s/cm}^2$ ]	$\log F_X$ [ $\text{erg/s/cm}^2$ ]
PM I00054-3721	M1.5	3575	4.34	-7.37	-13.01
PM I00115+5908	M5.5	2936	9.23	-9.33	-13.20
PM I00154-1608	M4.0	3165	4.99	-8.44	-13.41
PM I00184+4401	M3.5	3241	3.56	-8.01	-11.89
PM I01025+7140	M3.0	3318	8.24	-8.58	-13.19
PM I01026+6220	M1.5	3575	9.96	-8.10	-13.27
PM I01103-6726	M2.0	3500	8.20	-8.09	-12.87

Table 1: Excerpt of stellar parameters given by [Stelzer et al. \(2013\)](#). The total sample number is 159, with spectral types ranging from M0 to M8. Distance, effective temperature as well as bolometric and X-ray flux are needed for the computation. The full list of stellar parameters for the sample can be found as supplementary data to the article.

Coefficient	RG	MG	RV	EM
$S_{\text{eff},\odot}$	1.107	0.356	1.776	0.32
a	1.332e-4	6.171e-5	2.136e-4	5.547e-5
b	1.580e-8	1.698e-9	2.533e-8	1.526e-9
c	-8.308e-12	-3.198e-12	-1.332e-11	-2.874e-12
d	-1.931e-15	-5.575e-16	-3.097e-15	-5.011e-16

Table 2: Coefficients needed to determine the habitable zone for a planet with  $1 M_{\oplus}$  taken from [Kopparapu et al. \(2014\)](#), following different estimation for the distance (RG = runaway greenhouse, MG = maximum greenhouse, RV = recent venus and EM = early mars).

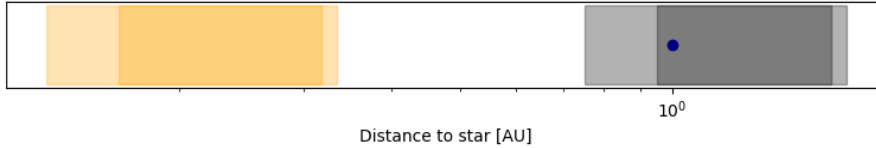


Figure 3: Comparison between the edges of the habitable zone around our Sun (grey) and around the star PM I00054-3721 from the sample (orange). The position of Earth is marked in blue for reference. The distances were computed following Kopparapu et al. (2014), lighter (darker) areas denote the optimistic (conservative) constraints. This figure shows the much closer proximity of the habitable zone to dM stars.

The stellar parameters from Stelzer et al. (2013) only include data for X-ray fluxes, so an estimation for the amount of EUV radiation coming from the stars in the sample has to be made. Even though the spectral energy distributions of M dwarfs differ quite significantly from the SED of solar-like stars (e.g. Wunderlich et al. 2019), the EUV emission of active M dwarfs can be estimated following the predictions of Tu et al. (2015) for the X-ray luminosities and corresponding EUV luminosities of active solar-like stars. In this case,  $L_{\text{EUV}}$  is estimated to be  $3L_X$  and therefore  $L_{\text{XUV}} = 4L_X$ , where the X-ray range from Tu et al. (2015) is given as  $\sim 0.1 - 10$  nm which, for the purposes of this approximation, corresponds to the EUV range of  $\sim 0.6 - 6$  nm from Stelzer et al. (2013). Using the distances for the habitable zone, the incident XUV flux on a planet can be calculated using Equation 4.1 to determine  $F_{\text{XUV}}$ , and the atmospheric loss follows from Equation 4.2. Assuming an atmospheric mass of  $M_{\oplus,\text{atm}} = 5.1 \times 10^{21}$  g (Williams 2019), the resulting loss rates can be used to calculate the time an Earth-like atmosphere could be sustained in orbit around these sample stars without considering possible mitigating factors such as e.g. outgassing from the planetary interior.

## 4.2 Results

Values for the mass-loss rates resulting from the computations illustrated in Section 4.1 together with the stellar XUV luminosity, habitable zone distances and retention time-scales are listed in Table 3. In general, dM stars are less luminous than solar-like stars (Reid & Hawley 2005, p. 169), which implies less irradiation for a planet that would orbit at a distance of 1 AU. However, this lower luminosity also results in a closer proximity of the habitable zone to the host star. Figure 3 illustrates this with a comparison between the habitable zone of a dM star from the sample and the habitable zone of our Sun. The calculated distances of the habitable zone in the sample attest to this, being on average 10 times closer to the host star than the distance between the Earth and the Sun. These closer orbits greatly enhance the incoming high-energy radiation on the planet, which follows Equation 4.1. As pointed out by e.g. Airapetian et al. (2017), the incident XUV radiation on planets in the habitable zones around active M dwarfs is up to 4 order of

magnitude higher than on Earth today. Figure 4 illustrates the incident XUV flux at the edges of the conservative and optimistic habitable zone respectively, given in terms of the incident flux on Earth today with a value of  $F_{\text{XUV, Earth}} = 5.6 \text{ erg s}^{-1} \text{ cm}^{-2}$  ([Airapetian et al. 2017](#)). Most of the stars in this sample return values that are between 1 and 3 orders of magnitude higher than the earth-equivalent (depending on the position of the orbit), but the maximum value of incident XUV flux shows an increase of about 4 orders of magnitude.

This increased amount of radiation leads to high rates of atmospheric mass loss, plotted in Figure 5 against the XUV luminosities of the host stars. Depending on the position of the planet with respect to the star (following the different boundaries for the habitable zone), the loss rates vary between  $\sim 10^7 - 10^{11} \text{ g s}^{-1}$ . These do not allow the retention of an Earth-like atmosphere over reasonable timescales, which are plotted in Figure 6 with respect to the XUV luminosity. Even under the most optimistic circumstances (where the planet orbits on the outer edge of the optimistic habitable zone), the most time it would take to lose the entire atmosphere of an Earth-like planet orbiting a star in this sample is  $\sim 85.9 \text{ Ma}$ . It follows that under the assumptions made here, none of the stars in the sample could house an Earth-like planet in their circumstellar habitable zones that would be able to retain its atmosphere given the star's XUV emission. When compared to the age-activity relation for M dwarfs given by [West et al. \(2008\)](#), it also becomes clear that, under the assumption that the stars in this sample are active M dwarfs, the amount of XUV radiation reaching the planet would not significantly change until the atmosphere is completely lost, since the activity-lifetimes of dM stars are multiple orders of magnitude longer than the time it takes these planets to lose their atmosphere entirely.

As discussed above, these loss rates have been computed using the energy-limited mass loss equation, which assumes a hydrodynamic outflow of atmospheric constituents through the absorption of incoming high-energy radiation. These results can be compared to the loss rates derived by [Lichtenegger et al. \(2010\)](#), where they calculated the loss of nitrogen atoms for Earth's present-day atmosphere when exposed to high amounts of XUV radiation ( $\leq 90 \text{ nm}$  in their case), while also taking the interaction with the solar wind as well as the varying size of the planetary magnetosphere as a protective layer for the atmosphere into account. [Lichtenegger et al. \(2010\)](#) assumed different amounts of incident XUV radiation (7, 10 and 20 times current solar value on Earth) and corresponded these to different stages of the solar evolution, therefore scaling the planetary magnetic moment and the solar wind parameters. For many of the potential planets around the stars in the sample used for the calculation here, the incident XUV radiation is much higher than 20 times the current solar value, but even with the loss values from [Lichtenegger et al. \(2010\)](#) as a lower limit, these planetary atmospheres would not survive longer than a few million years, effectively not changing the result that the stars in this sample do not provide an environment that would allow an Earth-like exoplanet to retain its atmosphere over extended periods of time.

Some of the planets, mainly on the outer orbits of the respective stellar habitable zone, receive amounts of XUV radiation that are comparable to Earth or even slightly below that, and it should also be noted that, as pointed out by [Stelzer et al. \(2013\)](#), around

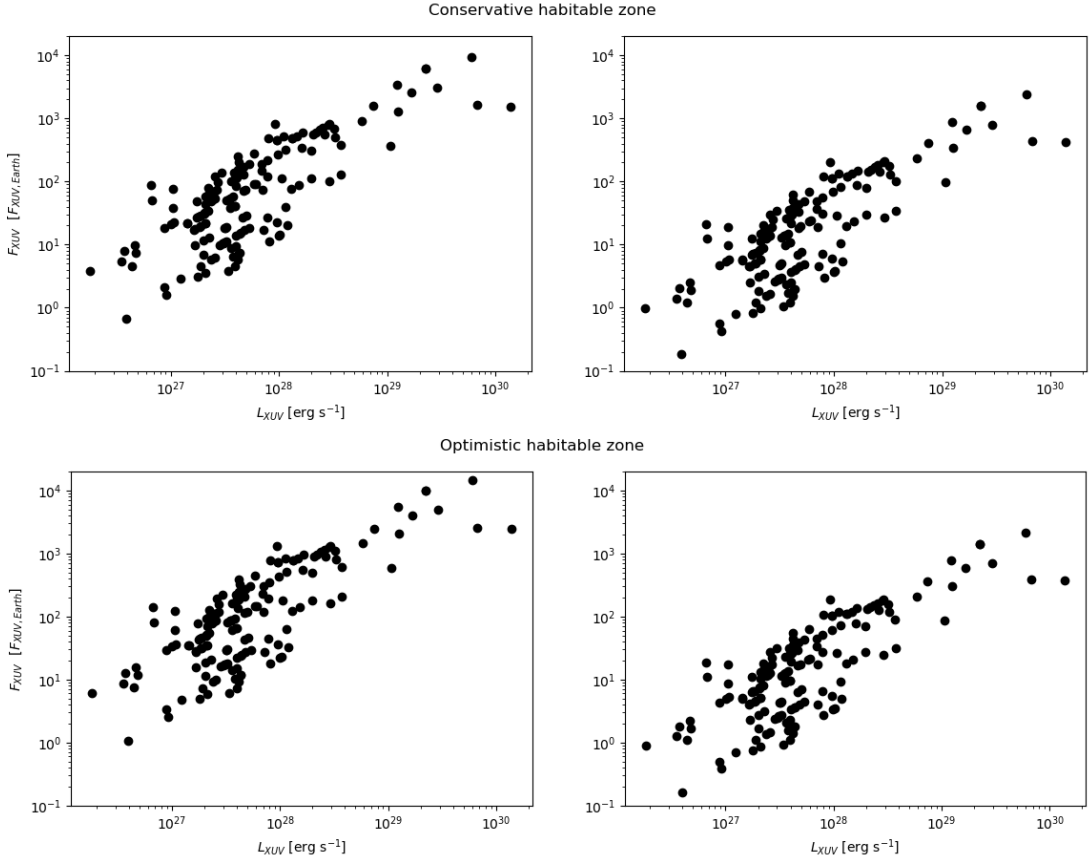


Figure 4: Incident XUV flux  $F_{XUV}$  in units of corresponding incident flux on Earth (value taken from [Airapetian et al. \(2017\)](#)) plotted with respect to the stellar XUV luminosity  $L_{XUV}$  for all stars in the sample given by [Stelzer et al. \(2013\)](#). The two figures on the left side assume an orbit at the respective inner edge of the habitable zone described by [Selsis et al. \(2007\)](#) while the two plots on the right side assume the orbit to be on the respective outer edge.

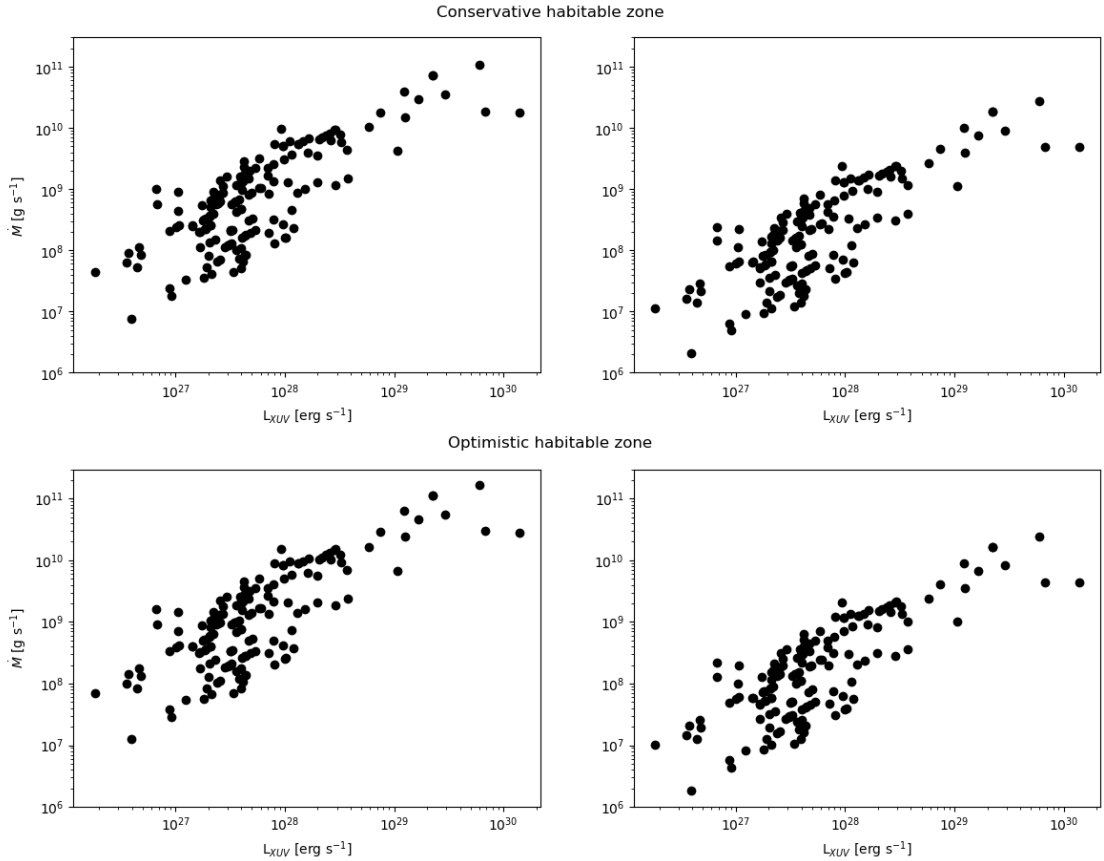


Figure 5: Atmospheric mass loss  $\dot{M}$  in units of  $\text{g s}^{-1}$  plotted with respect to the stellar XUV luminosity  $L_{\text{XUV}}$  for all star in the sample given by Stelzer et al. (2013). The distances to the potential planet in orbit have been computed with the equation for the borders of the habitable zone given by Kopparapu et al. (2014). The two plots on the left side of the figure assume the planet to orbit on the respective inner edge of the habitable zone, the two plots on the right side assume an orbit on the respective outer edge.

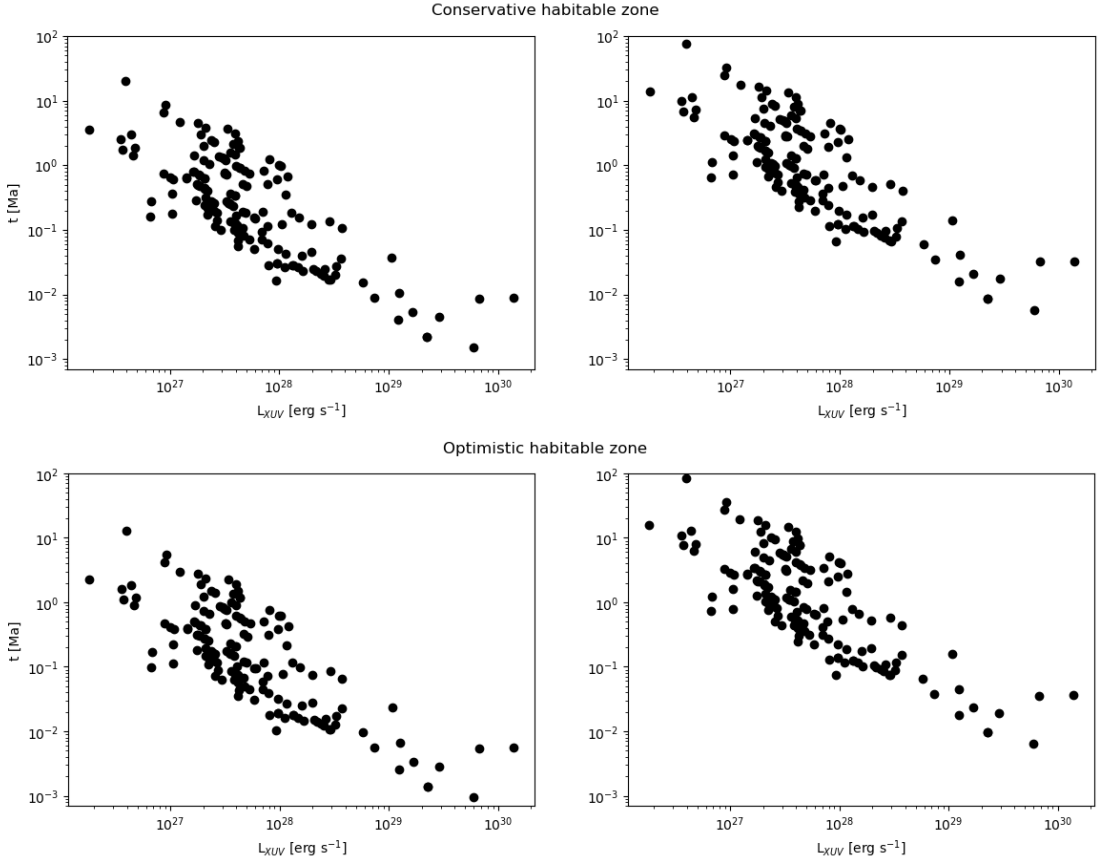


Figure 6: Retention time  $t$  in units of Ma for the atmosphere of an Earth-like planet plotted with respect to the stellar XUV luminosity  $L_{XUV}$  for all stars in the sample given by Stelzer et al. (2013). The two plots on the left side of the figure assume an orbit on the respective inner edge of the habitable zone described by Selsis et al. (2007), the two plots on the right side assume the orbit to be on the respective outer edge.

40% of the stars in the sample had no corresponding X-ray source when cross-referencing the sample to the different data sources, so the X-ray flux was obtained by estimating an upper limit through the sensitivity threshold of the *ROSAT All Sky Survey*. Since there is no actual data on the X-ray flux of these stars, it would theoretically be possible for them to have a high-energy flux that is low enough to allow an Earth-like planet orbiting in their habitable zone to retain its nitrogen-dominated atmosphere regarding the aspect of thermal loss, as it would be for the planets on the outer habitable zone boundaries mentioned above. However, even at reduced XUV levels that are comparable to our Sun, such as from Proxima Centauri (Güdel et al. 2004), the mass loss through non-thermal processes like the polar outflow of ions is most likely still high enough to not allow a potential planet to retain its atmosphere (Airapetian et al. 2017; Garcia-Sage et al. 2017).

## 5 Conclusion

Exoplanets situated in the habitable zone of M dwarf stars are subject to a stellar environment that is substantially different to the environment Earth resides in while orbiting the Sun. The strong stellar magnetic fields and the stellar activity linked to them, together with the proximity of the habitable zone to a dM host star can have such detrimental effects on the atmospheres of potential exoplanets that they might be stripped away on very short timescales, effectively making the affected planet inhospitable. This atmospheric loss happens through the thermal mechanisms of Jeans and hydrodynamic escape as well as through the non-thermal processes of sputtering, ion pick-up and polar flow. Nevertheless, M dwarfs are prime targets for scientific missions searching for exoplanets such as TESS, i.e. because the probability of detecting a transit is enhanced when observing dM stars since their planetary companions have shorter orbital periods and the fraction of stellar light blocked during the transit is significantly larger.

In analyzing the high-energy radiation environments of a sample of M dwarfs in this thesis, it becomes clear that none of these stars could support the nitrogen-dominated atmosphere of an Earth-like exoplanet over reasonable timescales. The thermal atmospheric loss instigated by the high amounts of XUV insolation that these planets experience leads to atmospheric retention timescales of around 1 Ma, rendering the planets inhospitable almost instantaneously on cosmic timescales. Even when only considering the non-thermal loss as a lower boundary of the loss rates, these atmospheres would likely survive less than 10 Ma, effectively not changing the result that these planets could not be considered habitable. An enhanced presence of CO<sub>2</sub> in the atmosphere would also lower the thermal loss rates due to its effective cooling, but such an atmosphere would resemble Venus more than Earth and the habitability of a planet with a CO<sub>2</sub>-dominated atmosphere is questionable.

Even though M dwarfs stand out amongst other stellar types i.e. through their long main sequence lifetimes during which they show no significant brightening and the fact that lower mass dM stars never evolve through the red giant phase, they might only be able to provide reasonable environments for the atmospheres of planets in their habitable zone after the end of their rather long activity lifetime and the enhanced atmospheric loss coupled to that. This implies that planets in orbit around them would either have to be able to protect their atmospheres during active phase of their stellar host, or that the volatile inventory of the planet must be sufficient to form an atmosphere after the end of the stellar activity.

Table 3: XUV-luminosities  $L_{\text{XUV}}$ , distances to the habitable zone  $d$ , mass loss rates  $\dot{M}$  and loss-timescales  $t$  for all stars in the sample by Stelzer et al. (2013). *Cons.* and *Opt.* refers to conservative and optimistic confirming assumptions described by Selsis et al. (2007), where the conservative assumptions are based on the runaway and maximum greenhouse effect and the optimistic assumptions are based on the *recent venus* an *early mars* criteria.

ID	$\log L_{\text{XUV}}$ [erg s <sup>-1</sup> ]	$d$ [AU]	$\log \dot{M}$ [g s <sup>-1</sup> ]	$t$ [Ma]
	<i>Cons.</i>	<i>Opt.</i>	<i>Cons.</i>	<i>Opt.</i>
PM I00054-3721	26.95	[0.16,0.32]	[0.13,0.33]	[7.38,6.80]
PM I00115+5908	27.41	[0.04,0.07]	[0.03,0.08]	[9.14,8.54]
PM I00154-1608	26.67	[0.06,0.11]	[0.04,0.12]	[8.04,7.45]
PM I00184+4401	27.89	[0.06,0.13]	[0.05,0.13]	[9.13,8.55]
PM I01025+7140	27.32	[0.08,0.15]	[0.06,0.16]	[8.40,7.82]
PM I01026+6220	27.41	[0.16,0.31]	[0.13,0.33]	[7.85,7.27]
PM I01103-6726	27.64	[0.14,0.26]	[0.11,0.28]	[8.24,7.66]
PM I01125-1659	27.40	[0.05,0.10]	[0.04,0.10]	[8.90,8.31]
PM I01510-0607	28.06	[0.05,0.10]	[0.04,0.10]	[9.56,8.97]
PM I02002+1303	27.90	[0.05,0.09]	[0.04,0.10]	[9.40,8.81]
PM I02022+1020	27.62	[0.03,0.07]	[0.03,0.07]	[9.45,8.85]
PM I02050-1736	28.18	[0.10,0.20]	[0.08,0.21]	[9.01,8.43]
PM I02058-3010	27.51	[0.10,0.20]	[0.08,0.22]	[8.33,7.75]
PM I02164+1335	27.77	[0.04,0.07]	[0.03,0.08]	[9.50,8.90]
PM I02336+2455	28.51	[0.05,0.11]	[0.04,0.11]	[9.89,9.30]
PM I02362+0652	27.61	[0.06,0.11]	[0.04,0.12]	[8.98,8.39]
PM I02365-5928	28.17	[0.04,0.08]	[0.03,0.09]	[9.78,9.18]
PM I02442+2531	27.85	[0.08,0.15]	[0.06,0.16]	[8.92,8.34]

Table 3: (Continued)

ID	$\log L_{\text{XUV}}$ [erg s <sup>-1</sup> ]	d [AU]			$\log \dot{M}$ [g s <sup>-1</sup> ]			t [Ma] Opt.
		Cons.	Opt.	Cons.	Opt.	Cons.	Opt.	
PM I02530+1652	26.82	[0.02,0.04]	[0.02,0.05]	[9.00,8.38]	[9.20,8.34]	[0.16,0.66]	[0.10,0.73]	
PM I03018-1635	28.57	[0.08,0.15]	[0.06,0.16]	[9.64,9.06]	[9.85,9.01]	[0.04,0.14]	[0.02,0.15]	
PM I03133+0446S	27.43	[0.04,0.08]	[0.03,0.09]	[9.05,8.45]	[9.26,8.41]	[0.14,0.56]	[0.09,0.62]	
PM I03507-0605	27.54	[0.06,0.13]	[0.05,0.13]	[8.78,8.20]	[8.99,8.15]	[0.26,1.01]	[0.16,1.12]	
PM I03526+1701	27.35	[0.05,0.09]	[0.04,0.10]	[8.85,8.26]	[9.06,8.21]	[0.22,0.87]	[0.14,0.97]	
PM I04311+5858	26.94	[0.06,0.11]	[0.04,0.11]	[8.32,7.73]	[8.53,7.69]	[0.75,2.94]	[0.47,3.27]	
PM I04429+1857	27.90	[0.14,0.26]	[0.11,0.28]	[8.50,7.92]	[8.70,7.87]	[0.51,1.91]	[0.32,2.12]	
PM I05019-0656	27.84	[0.05,0.11]	[0.04,0.11]	[9.22,8.63]	[9.43,8.59]	[0.09,0.37]	[0.06,0.41]	
PM I05033-1722	27.60	[0.08,0.15]	[0.06,0.16]	[8.67,8.09]	[8.88,8.04]	[0.34,1.29]	[0.21,1.43]	
PM I05085-1810	27.78	[0.06,0.13]	[0.05,0.13]	[9.02,8.44]	[9.23,8.39]	[0.15,0.58]	[0.09,0.65]	
PM I05116-4501	26.59	[0.19,0.37]	[0.15,0.39]	[6.89,6.32]	[7.09,6.27]	[20.52,76.27]	[12.79,84.86]	
PM I05280+0938	27.58	[0.06,0.13]	[0.05,0.13]	[8.82,8.24]	[9.03,8.19]	[0.24,0.92]	[0.15,1.02]	
PM I05421+1229	26.57	[0.05,0.11]	[0.04,0.11]	[7.95,7.36]	[8.16,7.32]	[1.77,6.88]	[1.10,7.66]	
PM I06000+0242	28.42	[0.05,0.11]	[0.04,0.11]	[9.80,9.21]	[10.01,9.17]	[0.02,0.10]	[0.02,0.11]	
PM I06011+5935	27.54	[0.06,0.13]	[0.05,0.13]	[8.78,8.20]	[8.99,8.15]	[0.26,1.01]	[0.16,1.12]	
PM I06024+4951	27.68	[0.04,0.08]	[0.03,0.09]	[9.29,8.69]	[9.50,8.65]	[0.08,0.32]	[0.05,0.36]	
PM I06103+8206	27.60	[0.13,0.26]	[0.11,0.28]	[8.21,7.63]	[8.41,7.58]	[0.99,3.72]	[0.61,4.14]	
PM I06105-2151	27.62	[0.21,0.41]	[0.17,0.43]	[7.82,7.25]	[8.02,7.21]	[2.41,8.87]	[1.50,9.87]	
PM I06246+2325	27.56	[0.05,0.09]	[0.04,0.10]	[9.06,8.47]	[9.27,8.42]	[0.14,0.54]	[0.09,0.60]	
PM I06307-7643	27.91	[0.03,0.07]	[0.03,0.07]	[9.74,9.14]	[9.95,9.09]	[0.03,0.12]	[0.02,0.13]	
PM I06337-7537N	28.03	[0.08,0.15]	[0.06,0.16]	[9.10,8.52]	[9.31,8.47]	[0.12,0.48]	[0.08,0.53]	

Table 3: (Continued)

ID	$\log L_{\text{XUV}}$ [erg s <sup>-1</sup> ]	d [AU]			$\dot{M}$ [g s <sup>-1</sup> ]			t [Ma] Opt.
		Cons.	Opt.	Cons.	Opt.	Cons.	Opt.	
PM I06337-7537S	28.06	[0.14,0.26]	[0.11,0.28]	[8.66,8.08]	[8.86,8.03]	[0.35,1.32]	[0.22,1.47]	
PM I06523-0511	27.49	[0.13,0.26]	[0.11,0.28]	[8.10,7.52]	[8.30,7.47]	[1.27,4.79]	[0.79,5.33]	
PM I06548+3316	26.64	[0.08,0.15]	[0.06,0.16]	[7.72,7.14]	[7.93,7.09]	[2.99,11.49]	[1.86,12.78]	
PM I06577-4417	27.22	[0.08,0.15]	[0.06,0.16]	[8.29,7.71]	[8.50,7.66]	[0.80,3.09]	[0.50,3.44]	
PM I07039+5242	27.73	[0.04,0.08]	[0.03,0.09]	[9.34,8.74]	[9.55,8.70]	[0.07,0.29]	[0.04,0.32]	
PM I07100+3831	28.38	[0.05,0.09]	[0.04,0.10]	[9.88,9.29]	[10.09,9.24]	[0.02,0.08]	[0.01,0.09]	
PM I07274+0513	26.55	[0.06,0.13]	[0.05,0.13]	[7.79,7.21]	[8.00,7.16]	[2.55,9.86]	[1.59,10.97]	
PM I07364+0704	27.59	[0.04,0.08]	[0.03,0.09]	[9.20,8.60]	[9.41,8.56]	[0.10,0.39]	[0.06,0.44]	
PM I07446+0333	29.09	[0.05,0.09]	[0.04,0.10]	[10.59,10.00]	[10.80,9.95]	[0.00,0.02]	[0.00,0.02]	
PM I07519-0000	27.60	[0.05,0.09]	[0.04,0.10]	[9.10,8.51]	[9.31,8.46]	[0.13,0.49]	[0.08,0.55]	
PM I07582+4118	27.55	[0.06,0.13]	[0.05,0.13]	[8.79,8.21]	[9.00,8.16]	[0.25,0.99]	[0.16,1.10]	
PM I08119+0846	27.39	[0.05,0.09]	[0.04,0.10]	[8.89,8.30]	[9.10,8.25]	[0.20,0.80]	[0.13,0.89]	
PM I08126-2133	27.03	[0.05,0.11]	[0.04,0.11]	[8.41,7.82]	[8.62,7.78]	[0.61,2.39]	[0.38,2.66]	
PM I08161+0118	27.73	[0.14,0.26]	[0.11,0.28]	[8.33,7.75]	[8.53,7.70]	[0.75,2.82]	[0.47,3.14]	
PM I08298+2646	26.83	[0.03,0.06]	[0.02,0.06]	[8.76,8.15]	[8.96,8.11]	[0.28,1.11]	[0.17,1.24]	
PM I08413+5929	27.63	[0.04,0.07]	[0.03,0.08]	[9.36,8.76]	[9.57,8.71]	[0.07,0.27]	[0.04,0.31]	
PM I08582+1945N	28.05	[0.04,0.07]	[0.03,0.08]	[9.78,9.18]	[9.99,9.13]	[0.03,0.10]	[0.02,0.12]	
PM I08589+0828	29.22	[0.06,0.13]	[0.05,0.13]	[10.46,9.88]	[10.67,9.83]	[0.01,0.02]	[0.00,0.02]	
PM I09170-7749	27.32	[0.05,0.09]	[0.04,0.10]	[8.82,8.23]	[9.03,8.18]	[0.24,0.94]	[0.15,1.04]	
PM I09307+0019	27.67	[0.06,0.13]	[0.05,0.13]	[8.91,8.33]	[9.12,8.28]	[0.19,0.75]	[0.12,0.83]	
PM I09360-2139	27.50	[0.11,0.21]	[0.08,0.22]	[8.32,7.74]	[8.52,7.69]	[0.77,2.91]	[0.48,3.24]	

Table 3: (Continued)

ID	$\log L_{\text{XUV}}$	$d$ [AU]	$\dot{M}$ [ $\text{g s}^{-1}$ ]		Cons.	Opt.	$t$ [Ma]
	[ $\text{erg s}^{-1}$ ]	Cons.	Opt.	Cons.	Opt.	Cons.	Opt.
PM I09397-4104	28.57	[0.13,0.26]	[0.11,0.28]	[9.18,8.60]	[9.38,8.55]	[0.11,0.40]	[0.07,0.44]
PM I09444-4546	27.58	[0.19,0.37]	[0.15,0.39]	[7.87,7.30]	[8.07,7.25]	[2.15,7.99]	[1.34,8.89]
PM I09539+2056	27.67	[0.05,0.09]	[0.04,0.10]	[9.17,8.58]	[9.38,8.53]	[0.11,0.42]	[0.07,0.47]
PM I10122-0344	27.98	[0.16,0.32]	[0.13,0.33]	[8.42,7.84]	[8.62,7.80]	[0.61,2.27]	[0.38,2.53]
PM I10196+1952	29.10	[0.08,0.15]	[0.06,0.16]	[10.17,9.59]	[10.38,9.54]	[0.01,0.04]	[0.01,0.05]
PM I10289+0050	27.48	[0.14,0.26]	[0.11,0.28]	[8.08,7.50]	[8.28,7.45]	[1.33,5.02]	[0.83,5.58]
PM I10482-1120	27.02	[0.03,0.06]	[0.02,0.06]	[8.95,8.34]	[9.15,8.30]	[0.18,0.72]	[0.11,0.80]
PM I10497+3532	27.62	[0.05,0.09]	[0.04,0.10]	[9.12,8.53]	[9.33,8.48]	[0.12,0.47]	[0.07,0.52]
PM I10508+0648	27.39	[0.05,0.11]	[0.04,0.11]	[8.77,8.18]	[8.98,8.14]	[0.27,1.04]	[0.17,1.16]
PM I11000+2249	27.67	[0.11,0.20]	[0.08,0.22]	[8.49,7.91]	[8.69,7.86]	[0.52,1.97]	[0.32,2.19]
PM I11033+3558	27.51	[0.13,0.26]	[0.11,0.28]	[8.12,7.54]	[8.32,7.49]	[1.21,4.58]	[0.76,5.09]
PM I11054+4331	28.01	[0.21,0.41]	[0.17,0.44]	[8.21,7.64]	[8.41,7.60]	[0.98,3.62]	[0.61,4.02]
PM I11200+6550	27.53	[0.24,0.46]	[0.19,0.48]	[7.64,7.08]	[7.85,7.03]	[3.63,13.30]	[2.26,14.79]
PM I11354-3232	27.56	[0.16,0.31]	[0.13,0.33]	[8.00,7.42]	[8.20,7.38]	[1.60,5.98]	[0.99,6.65]
PM I11476+7841	27.16	[0.06,0.13]	[0.05,0.13]	[8.40,7.82]	[8.61,7.77]	[0.63,2.42]	[0.39,2.69]
PM I11477+0048	27.32	[0.06,0.11]	[0.04,0.11]	[8.70,8.11]	[8.91,8.07]	[0.31,1.22]	[0.20,1.36]
PM I11509+4822	27.60	[0.05,0.09]	[0.04,0.10]	[9.10,8.51]	[9.31,8.46]	[0.13,0.49]	[0.08,0.55]
PM I11511+3516	28.08	[0.19,0.37]	[0.15,0.39]	[8.37,7.80]	[8.57,7.75]	[0.68,2.53]	[0.42,2.81]
PM I12142+0037	28.22	[0.04,0.08]	[0.03,0.09]	[9.83,9.23]	[10.04,9.19]	[0.02,0.09]	[0.01,0.10]
PM I12189+1107	28.12	[0.04,0.08]	[0.03,0.09]	[9.74,9.14]	[9.95,9.10]	[0.03,0.11]	[0.02,0.13]
PM I12248-1814	27.64	[0.13,0.26]	[0.11,0.28]	[8.25,7.67]	[8.45,7.62]	[0.90,3.39]	[0.56,3.77]

Table 3: (Continued)

ID	$\log L_{\text{XUV}}$	$d$ [AU]	$\dot{M}$ [ $\text{g s}^{-1}$ ]	Cons.	Opt.	Cons.	Opt.	Cons.	Opt.	t [Ma]
	[ $\text{erg s}^{-1}$ ]			[ $\text{erg s}^{-1}$ ]		[ $\text{erg s}^{-1}$ ]		[ $\text{erg s}^{-1}$ ]		
PM II2332+0901	28.12	[0.04,0.08]	[0.03,0.09]	[9.74,9.14]	[9.95,9.10]	[0.03,0.11]	[0.02,0.13]			
PM II2378-5200	28.46	[0.13,0.26]	[0.11,0.28]	[9.07,8.49]	[9.27,8.44]	[0.14,0.51]	[0.08,0.57]			
PM II2388-3822	27.40	[0.05,0.09]	[0.04,0.10]	[8.90,8.31]	[9.11,8.26]	[0.20,0.78]	[0.12,0.87]			
PM II2407-4333	27.55	[0.08,0.15]	[0.06,0.16]	[8.63,8.05]	[8.84,8.00]	[0.37,1.41]	[0.23,1.57]			
PM II2479+0945	27.26	[0.06,0.13]	[0.05,0.13]	[8.50,7.92]	[8.71,7.87]	[0.50,1.92]	[0.31,2.14]			
PM II3005+0541	28.34	[0.05,0.09]	[0.04,0.10]	[9.84,9.25]	[10.05,9.20]	[0.02,0.09]	[0.01,0.10]			
PM II3299+1022	27.91	[0.21,0.41]	[0.17,0.43]	[8.11,7.54]	[8.31,7.50]	[1.23,4.55]	[0.77,5.06]			
PM II3427+3317	27.35	[0.06,0.13]	[0.05,0.13]	[8.59,8.01]	[8.80,7.96]	[0.40,1.56]	[0.25,1.74]			
PM II4342-1231	27.38	[0.06,0.11]	[0.04,0.11]	[8.75,8.16]	[8.96,8.12]	[0.28,1.09]	[0.17,1.21]			
PM II4495-2606E	26.96	[0.19,0.37]	[0.15,0.39]	[7.26,6.69]	[7.46,6.64]	[8.75,32.54]	[5.46,36.20]			
PM II4544+1606	29.03	[0.14,0.26]	[0.11,0.28]	[9.63,9.05]	[9.83,9.00]	[0.04,0.14]	[0.02,0.16]			
PM II4574-2124W	27.32	[0.19,0.37]	[0.15,0.39]	[7.62,7.05]	[7.82,7.00]	[3.82,14.20]	[2.38,15.80]			
PM II5194-0743E	27.27	[0.08,0.15]	[0.06,0.16]	[8.34,7.76]	[8.55,7.71]	[0.72,2.76]	[0.45,3.07]			
PM II5322-4116	27.52	[0.11,0.20]	[0.08,0.22]	[8.34,7.76]	[8.54,7.71]	[0.73,2.78]	[0.46,3.10]			
PM II6028+2035	27.41	[0.05,0.11]	[0.04,0.11]	[8.79,8.20]	[9.00,8.16]	[0.26,1.00]	[0.16,1.11]			
PM II6200-3731E	27.68	[0.13,0.26]	[0.11,0.28]	[8.29,7.71]	[8.49,7.66]	[0.82,3.09]	[0.51,3.44]			
PM II6241+4821	27.22	[0.10,0.20]	[0.08,0.22]	[8.05,7.47]	[8.25,7.42]	[1.43,5.43]	[0.89,6.04]			
PM II6254+5418	27.38	[0.16,0.31]	[0.13,0.33]	[7.82,7.24]	[8.02,7.20]	[2.42,9.05]	[1.51,10.07]			
PM II6303-1239	27.31	[0.06,0.13]	[0.05,0.13]	[8.56,7.98]	[8.77,7.93]	[0.43,1.68]	[0.27,1.86]			
PM II6313+4051	27.02	[0.04,0.08]	[0.03,0.09]	[8.64,8.04]	[8.85,8.00]	[0.36,1.43]	[0.23,1.59]			
PM II6554-0819	27.31	[0.06,0.13]	[0.05,0.13]	[8.55,7.97]	[8.76,7.92]	[0.44,1.71]	[0.28,1.91]			

Table 3: (Continued)

ID	$\log L_{\text{XUV}}$	$d$ [AU]	$\dot{M}$ [ $\text{g s}^{-1}$ ]	Cons.	Opt.	Cons.	Opt.	Cons.	Opt.	$t$ [Ma]
	[ $\text{erg s}^{-1}$ ]									
PM II6554-0820	29.46	[0.08,0.15]	[0.06,0.16]	[10.54,9.96]	[10.75,9.91]	[0.00,0.02]	[0.00,0.02]	[0.00,0.02]	[0.00,0.02]	[0.00,0.02]
PM II6555-0823	27.97	[0.03,0.05]	[0.02,0.06]	[9.98,9.37]	[10.18,9.32]	[0.02,0.07]	[0.02,0.07]	[0.01,0.08]	[0.01,0.08]	[0.01,0.08]
PM II6570-0420	28.77	[0.06,0.13]	[0.05,0.13]	[10.01,9.43]	[10.22,9.38]	[0.02,0.06]	[0.02,0.06]	[0.01,0.07]	[0.01,0.07]	[0.01,0.07]
PM II7033+5124	27.36	[0.05,0.10]	[0.04,0.10]	[8.86,8.27]	[9.07,8.22]	[0.22,0.85]	[0.22,0.85]	[0.14,0.95]	[0.14,0.95]	[0.14,0.95]
PM II7095+4340	27.15	[0.06,0.13]	[0.05,0.13]	[8.39,7.81]	[8.60,7.76]	[0.64,2.48]	[0.64,2.48]	[0.40,2.76]	[0.40,2.76]	[0.40,2.76]
PM II7121+4539	27.69	[0.06,0.13]	[0.05,0.13]	[8.93,8.35]	[9.14,8.30]	[0.18,0.71]	[0.18,0.71]	[0.12,0.79]	[0.12,0.79]	[0.12,0.79]
PM II7286-4653	28.11	[0.10,0.20]	[0.08,0.22]	[8.94,8.36]	[9.14,8.31]	[0.18,0.70]	[0.18,0.70]	[0.11,0.78]	[0.11,0.78]	[0.11,0.78]
PM II7303+0532	27.60	[0.24,0.45]	[0.19,0.48]	[7.71,7.15]	[7.92,7.10]	[3.09,11.32]	[3.09,11.32]	[1.93,12.59]	[1.93,12.59]	[1.93,12.59]
PM II7352-4840	27.86	[0.16,0.32]	[0.13,0.34]	[8.29,7.71]	[8.49,7.67]	[0.82,3.07]	[0.82,3.07]	[0.51,3.41]	[0.51,3.41]	[0.51,3.41]
PM II7364+6820	27.32	[0.08,0.15]	[0.06,0.16]	[8.40,7.82]	[8.61,7.77]	[0.62,2.40]	[0.62,2.40]	[0.39,2.67]	[0.39,2.67]	[0.39,2.67]
PM II7370-4419	26.68	[0.06,0.13]	[0.05,0.13]	[7.92,7.34]	[8.13,7.29]	[1.89,7.31]	[1.89,7.31]	[1.18,8.14]	[1.18,8.14]	[1.18,8.14]
PM II7378+1835	27.25	[0.19,0.37]	[0.15,0.39]	[7.55,6.98]	[7.75,6.93]	[4.49,16.69]	[4.49,16.69]	[2.80,18.56]	[2.80,18.56]	[2.80,18.56]
PM II7439+4322	27.70	[0.10,0.20]	[0.08,0.22]	[8.53,7.95]	[8.73,7.90]	[0.47,1.80]	[0.47,1.80]	[0.29,2.00]	[0.29,2.00]	[0.29,2.00]
PM II7464+2743W	28.52	[0.06,0.13]	[0.05,0.13]	[9.76,9.18]	[9.97,9.13]	[0.03,0.11]	[0.03,0.11]	[0.02,0.12]	[0.02,0.12]	[0.02,0.12]
PM II7465-5719	27.45	[0.13,0.26]	[0.11,0.28]	[8.06,7.48]	[8.26,7.43]	[1.39,5.26]	[1.39,5.26]	[0.87,5.85]	[0.87,5.85]	[0.87,5.85]
PM II7578+0441N	26.26	[0.05,0.11]	[0.04,0.11]	[7.64,7.05]	[7.85,7.01]	[3.61,14.06]	[3.61,14.06]	[2.25,15.64]	[2.25,15.64]	[2.25,15.64]
PM II8051-0301	27.64	[0.19,0.37]	[0.15,0.39]	[7.93,7.36]	[8.13,7.31]	[1.87,6.96]	[1.87,6.96]	[1.17,7.74]	[1.17,7.74]	[1.17,7.74]
PM II8075-1557	28.45	[0.05,0.09]	[0.04,0.10]	[9.96,9.37]	[10.17,9.32]	[0.02,0.07]	[0.02,0.07]	[0.01,0.08]	[0.01,0.08]	[0.01,0.08]
PM II8189+6611	27.84	[0.05,0.10]	[0.04,0.10]	[9.34,8.75]	[9.55,8.70]	[0.07,0.28]	[0.07,0.28]	[0.04,0.31]	[0.04,0.31]	[0.04,0.31]
PM II8224+6203	27.24	[0.05,0.09]	[0.04,0.10]	[8.74,8.15]	[8.95,8.10]	[0.29,1.13]	[0.29,1.13]	[0.18,1.25]	[0.18,1.25]	[0.18,1.25]
PM II8411+2447S	28.47	[0.05,0.09]	[0.04,0.10]	[9.97,9.38]	[10.18,9.33]	[0.02,0.07]	[0.02,0.07]	[0.01,0.07]	[0.01,0.07]	[0.01,0.07]

Table 3: (Continued)

ID	$\log L_{\text{XUV}}$	$d$ [AU]	$\log \dot{M}$ [ $\text{g s}^{-1}$ ]		t [Ma]	
	[ $\text{erg s}^{-1}$ ]	Cons.	Opt.	Cons.	Opt.	Cons.
PM II8427+5937N	27.28	[0.08,0.15]	[0.06,0.16]	[8.35,7.77]	[8.56,7.72]	[0.70,2.69]
PM II8427+5937S	27.25	[0.06,0.13]	[0.05,0.13]	[8.49,7.91]	[8.70,7.86]	[0.51,1.97]
PM II8498-2350	28.30	[0.06,0.13]	[0.05,0.13]	[9.54,8.96]	[9.75,8.91]	[0.05,0.18]
PM II9070+2053	27.28	[0.16,0.32]	[0.13,0.33]	[7.72,7.14]	[7.92,7.10]	[3.04,11.39]
PM II9072+2052	27.31	[0.14,0.26]	[0.11,0.28]	[7.91,7.33]	[8.11,7.28]	[1.97,7.42]
PM II9077+3232	27.60	[0.08,0.15]	[0.06,0.16]	[8.67,8.09]	[8.88,8.04]	[0.34,1.29]
PM II9169+0510	27.31	[0.11,0.21]	[0.08,0.22]	[8.13,7.55]	[8.33,7.50]	[1.19,4.51]
PM II9216+2052	27.43	[0.05,0.09]	[0.04,0.10]	[8.93,8.34]	[9.14,8.29]	[0.19,0.73]
PM II9539+4424E	27.98	[0.04,0.07]	[0.03,0.08]	[9.71,9.11]	[9.92,9.06]	[0.03,0.12]
PM II9539+4424W	27.98	[0.04,0.07]	[0.03,0.08]	[9.71,9.11]	[9.92,9.06]	[0.03,0.12]
PM I20260+5834	27.35	[0.04,0.08]	[0.03,0.09]	[8.96,8.36]	[9.17,8.32]	[0.17,0.68]
PM I20298+0941	28.41	[0.05,0.09]	[0.04,0.10]	[9.91,9.32]	[10.12,9.27]	[0.02,0.08]
PM I20305+6526	28.30	[0.10,0.20]	[0.08,0.22]	[9.12,8.54]	[9.32,8.49]	[0.12,0.46]
PM I20405+1529	27.59	[0.05,0.10]	[0.04,0.10]	[9.09,8.50]	[9.30,8.45]	[0.13,0.50]
PM I20451-3120	30.14	[0.24,0.46]	[0.19,0.48]	[10.25,9.69]	[10.46,9.64]	[0.01,0.03]
PM I20525-1658	27.22	[0.08,0.15]	[0.06,0.16]	[8.30,7.72]	[8.51,7.67]	[0.79,3.02]
PM I20533+6209	28.00	[0.21,0.41]	[0.17,0.43]	[8.20,7.63]	[8.40,7.59]	[1.00,3.70]
PM I21296+1738	27.27	[0.06,0.13]	[0.05,0.13]	[8.51,7.93]	[8.72,7.88]	[0.49,1.88]
PM I21313-0947	27.99	[0.05,0.09]	[0.04,0.10]	[9.49,8.90]	[9.70,8.85]	[0.05,0.20]
PM I21335-4900	27.09	[0.16,0.32]	[0.13,0.33]	[7.53,6.95]	[7.73,6.91]	[4.71,17.64]
PM I22012+2818	28.87	[0.05,0.11]	[0.04,0.11]	[10.25,9.66]	[10.46,9.62]	[0.01,0.03]

Table 3: (Continued)

ID	$\log L_{\text{XUV}}$ [erg s <sup>-1</sup> ]	d [AU]			$\log \dot{M}$ [g s <sup>-1</sup> ]			t [Ma]
		Cons.	Opt.	Cons.	Opt.	Cons.	Opt.	
PM I22024-3704	27.51	[0.06,0.13]	[0.05,0.13]	[8.75,8.17]	[8.96,8.12]	[0.28,1.08]	[0.17,1.20]	
PM I22096-0438	27.77	[0.06,0.13]	[0.05,0.13]	[9.01,8.43]	[9.22,8.38]	[0.15,0.59]	[0.10,0.66]	
PM I22231-1736	28.31	[0.05,0.10]	[0.04,0.10]	[9.81,9.22]	[10.02,9.17]	[0.02,0.10]	[0.02,0.11]	
PM I22387-2037	29.83	[0.16,0.32]	[0.13,0.33]	[10.27,9.69]	[10.47,9.65]	[0.01,0.03]	[0.01,0.04]	
PM I22468+4420	29.78	[0.06,0.13]	[0.05,0.13]	[11.02,10.44]	[11.23,10.39]	[0.00,0.01]	[0.00,0.01]	
PM I22532-1415	27.00	[0.06,0.11]	[0.04,0.11]	[8.38,7.79]	[8.59,7.75]	[0.66,2.56]	[0.41,2.85]	
PM I22557-7527	27.36	[0.11,0.21]	[0.08,0.22]	[8.18,7.60]	[8.38,7.55]	[1.06,4.02]	[0.66,4.48]	
PM I22565+1633	27.60	[0.16,0.32]	[0.13,0.33]	[8.04,7.46]	[8.24,7.42]	[1.46,5.45]	[0.91,6.07]	
PM I23318+1956E	29.35	[0.05,0.09]	[0.04,0.10]	[10.85,10.26]	[11.06,10.21]	[0.00,0.01]	[0.00,0.01]	
PM I23318+1956Wn	29.35	[0.05,0.09]	[0.04,0.10]	[10.85,10.26]	[11.06,10.21]	[0.00,0.01]	[0.00,0.01]	
PM I23351-0223	27.47	[0.04,0.07]	[0.03,0.08]	[9.20,8.60]	[9.41,8.55]	[0.10,0.40]	[0.06,0.44]	
PM I23419+4410	27.62	[0.04,0.08]	[0.03,0.09]	[9.24,8.64]	[9.45,8.60]	[0.09,0.36]	[0.06,0.40]	
PM I23431+3632	28.21	[0.05,0.11]	[0.04,0.11]	[9.59,9.00]	[9.80,8.96]	[0.04,0.16]	[0.03,0.18]	
PM I23492+0224	27.63	[0.19,0.37]	[0.15,0.39]	[7.93,7.36]	[8.13,7.31]	[1.87,6.96]	[1.17,7.74]	
PM I23538-7537	27.49	[0.14,0.26]	[0.11,0.28]	[8.09,7.51]	[8.29,7.46]	[1.30,4.90]	[0.81,5.46]	

## References

- Airapetian, V. S., Glocer, A., Khazanov, G. V., et al. 2017, ApJL, 836, L3
- Barnes, R., Mullins, K., Goldblatt, C., et al. 2013, Astrobiology, 13, 225
- Bauer, S. J. & Lammer, H. 2004, Planetary aeronomy: atmosphere environments in planetary systems, Physics of earth and space environments (Berlin [u.a.]: Springer-Verl.)
- Catling, D. C. & Zahnle, K. J. 2009, Scientific American, 300, 36
- Claire, M. W., Sheets, J., Cohen, M., et al. 2012, ApJ, 757, 95
- Cooper, K. 2018, The Astrobiology Magazine Guide to TESS, from <https://www.astrobio.net/news-exclusive/the-astrobiology-magazine-guide-to-tess/>, [Online; accessed 08-July-2019]
- CoRoT. 2016, CNES Project Library, from <https://corot.cnes.fr/en/COROT/index.htm>, [Online; accessed 12-July-2019]
- Elkins-Tanton, L. T. 2012, Annual Review of Earth and Planetary Sciences, 40, 113
- Exoplanet Catalogue. 2019, The Extrasolar Planets Encyclopedia, from <http://exoplanet.eu/catalog/>, [Online; accessed 29-June-2019]
- Fontenla, J. M., Linsky, J. L., Witbrod, J., et al. 2016, ApJ, 830, 154
- Garcia-Sage, K., Glocer, A., Drake, J. J., Gronoff, G., & Cohen, O. 2017, ApJL, 844, L13
- Güdel, M., Audard, M., Reale, F., Skinner, S. L., & Linsky, J. L. 2004, A&A, 416, 713
- Johnson, M. 2018, KEPLER Mission overview, from [https://www.nasa.gov/mission\\_pages/kepler/overview/index.html](https://www.nasa.gov/mission_pages/kepler/overview/index.html), [Online; accessed 03-July-2019]
- Johnstone, C. P., Khodachenko, M. L., Lüftinger, T., et al. 2019, A&A, 624, L10
- Kislyakova, K. G., Fossati, L., Johnstone, C. P., et al. 2018, ApJ, 858, 105
- Kislyakova, K. G., Johnstone, C. P., Odert, P., et al. 2014, A&A, 562, A116
- Kopparapu, R. K., Ramirez, R., Kasting, J. F., et al. 2013, ApJ, 765, 131
- Kopparapu, R. K., Ramirez, R. M., SchottelKotte, J., et al. 2014, ApJL, 787, L29
- Lammer, H., Zerkle, A. L., Gebauer, S., et al. 2018, A&ARv, 26, 2
- Laughlin, G., Bodenheimer, P., & Adams, F. C. 1997, ApJ, 482, 420
- Lichtenegger, H. I. M., Lammer, H., Grießmeier, J.-M., et al. 2010, Icarus, 210, 1

- NASA Exoplanet Archive. 2019, Exoplanet and Candidate Statistics, from [https://exoplanetarchive.ipac.caltech.edu/docs/counts\\_detail.html](https://exoplanetarchive.ipac.caltech.edu/docs/counts_detail.html), [Online; accessed 03-July-2019]
- Reid, I. N. & Hawley, S. L. 2005, New light on dark stars: red dwarfs, low mass stars, brown dwarfs, 2nd edn., Springer Praxis books in astrophysics and astronomy (Berlin [u.a.]: Springer Praxis Publ.)
- Renneboog, R. & Boorstein, M. 2013, Earth's weather, water, and atmosphere, Earth science (Ipswich, MA: Salem Press)
- Ricker, G. R., Vanderspek, R., Winn, J., et al. 2016, in Proc. SPIE, Vol. 9904, Space Telescopes and Instrumentation 2016: Optical, Infrared, and Millimeter Wave, 99042B
- Scalo, J., Kaltenegger, L., Segura, A. G., et al. 2007, Astrobiology, 7, 85
- Selsis, F., Kasting, J. F., Levrard, B., et al. 2007, A&A, 476, 1373
- Shields, A. L., Ballard, S., & Johnson, J. A. 2016, Physics Reports, 663, 1
- Stelzer, B., Marino, A., Micela, G., López-Santiago, J., & Liefke, C. 2013, MNRAS, 431, 2063
- TESS. 2019, Mission overview, from <https://tess.mit.edu/science/>, [Online; accessed 03-July-2019]
- Tian, F., Kasting, J. F., Liu, H.-L., & Roble, R. G. 2008, Journal of Geophysical Research (Planets), 113, E05008
- Tu, L., Johnstone, C. P., Güdel, M., & Lammer, H. 2015, A&A, 577, L3
- Vidotto, A. A., Jardine, M., Morin, J., et al. 2013, A&A, 557, A67
- West, A. A., Hawley, S. L., Bochanski, J. J., et al. 2008, ApJ, 135, 785
- Williams, D. 2019, Earth Fact Sheet, from <https://nssdc.gsfc.nasa.gov/planetary/factsheet/earthfact.html>, [Online; accessed 27-June-2019]
- Wunderlich, F., Godolt, M., Grenfell, J. L., et al. 2019, A&A, 624, A49
- Zahnle, K., Schaefer, L., & Fegley, B. 2010, Cold Spring Harb Perspect Biol, 2, a004895